



DEPARTMENT OF MARINE TECHNOLOGY (MSMIR)

TTK4250 - SENSOR FUSION

Guided Assignment 1: Report

Authors :

Madhushree Sannigrahi (Student Number: 128570)

Abhimanyu Bhowmik (Student Number: 128581)

October 2024

1 Task 5: ESKF on simulated data

Ans a:

The orientation graph (figure 1a) shows that the graph has high variability at the beginning, stabilizing at about 50 sec. After that, the error plot stabilizes at around $\pm 1\sigma$ bound but continues to have small perturbations. This might be due to low GNSS update frequency of 1Hz which makes the filter heavily reliant on IMU readings. The Gyro bias and accelerometer bias can also contribute to the slight drifts in orientation when left uncorrected for a long time. Referring to equation 10.56 in the book Brekke 2024, we see that the error-gyro bias also contributes to the fluctuations of the error orientation estimate. As in the Error-Gyro bias plot (figure 1b), we see that ω_{bz} has a slightly increased value at around 225-275 sec. This is also reflected in the Error Orientation plot (ω_ψ).

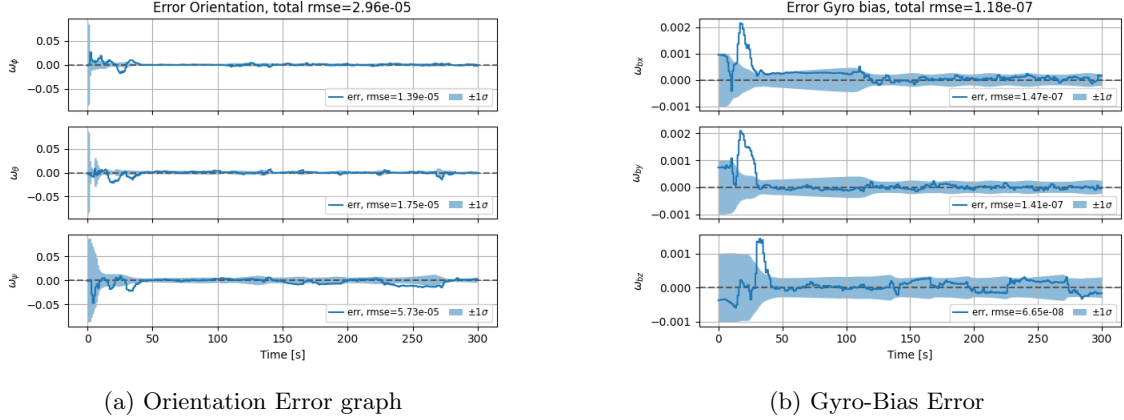


Figure 1: Graphs highlighting the role of Gyro Bias Error in Orientation Error

Ans b:

We also see in graph 1a that the orientation error is the greatest in yaw direction. This is because yaw is only dependent on the gyroscope, and unlike pitch/roll, it can't be determined by gravity using an accelerometer. Thus, Yaw is directly dependent on gyro_bias as well. Increasing the standard deviation of gyro_bias from $5e-5$ to $1e-4$ makes the filter "less confident" in its estimate of the gyroscope bias which leads to a greater increase in rmse in yaw direction of the orientation error than roll and pitch as can be seen in figure 2. This deviation in yaw direction can persist indefinitely if there is a persistent uncorrected gyroscopic bias as they can integrate over time and lead to large orientation errors. This can be mitigated if the update rate of GNSS is increased since high-frequency GNSS correction will reduce the chances of error accumulation.

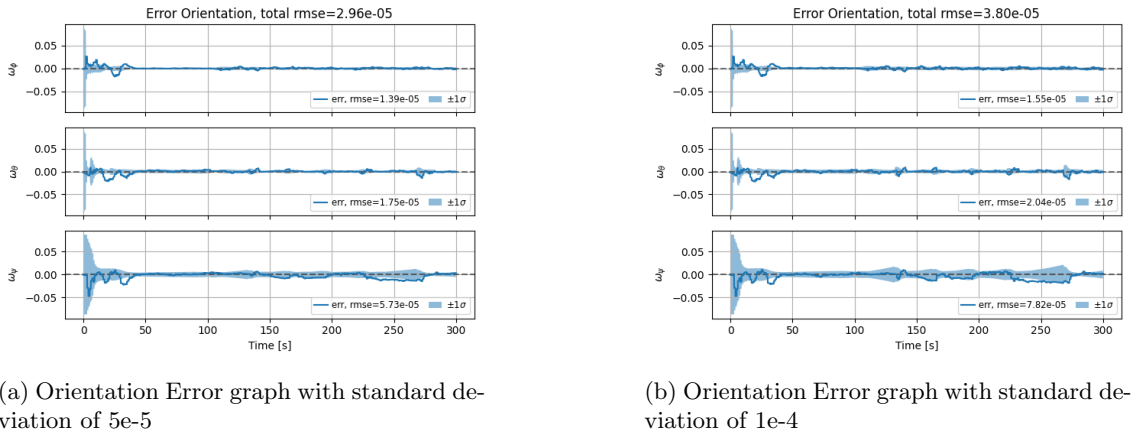


Figure 2: Graphs showing the affect on Orientation Error with increase in standard deviation in Gyro Bias

Ans c:

When we round off `accm_correction` and `gyrom_correction`, the filter performance degrades largely because by rounding them off, we eliminate the fine-grained corrections in accelerometer and gyro measurement, which then leads to residual errors. The accelerometer and gyro bias get much more error-prone without the corrections, and the IMU no longer represents the true motion of UAV as seen in figure 3(a)(c). If we look into the yaw direction of NEES value of Gyro-bias as in graph 3(d), it is much above the expected confidence bound than roll and pitch. The yaw-drift issue may have compounded due to loss of precision in `gyrom_correction`. This also explains the orientation drift in yaw-direction (figure 3(b)). Subsequently, there is a huge drift in the x and y of NEES accel bias in figure 3(f). This might be because the initial `accm_correction` was much higher in the x and y direction rather than z and rounding them off resulted in deviations.

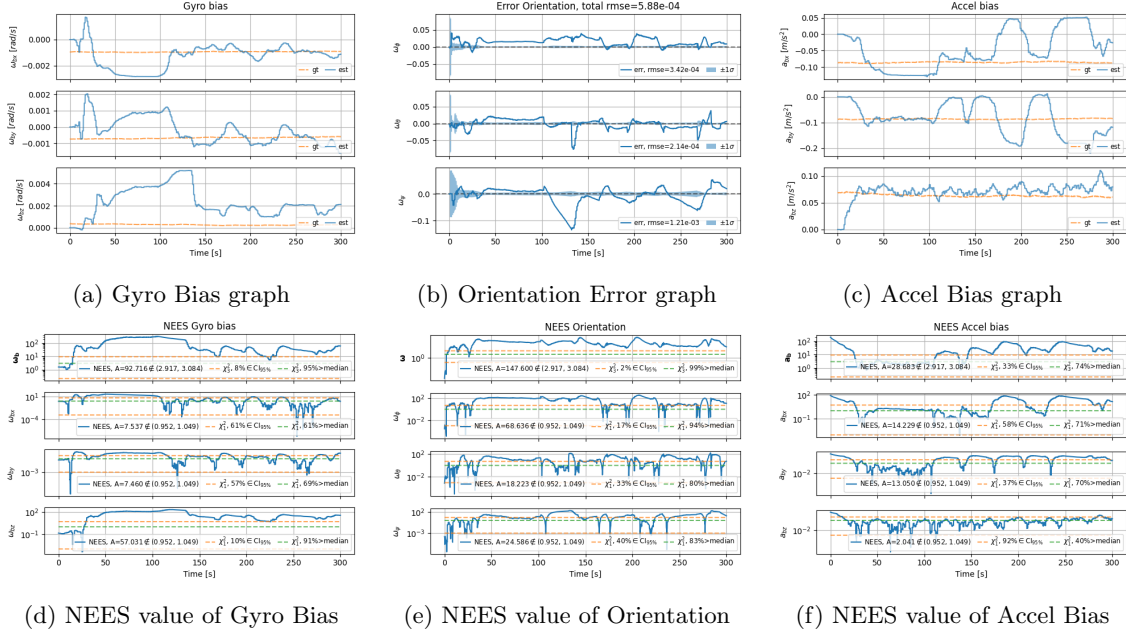


Figure 3: Graphs showing the effects of round off `accm_correction` and `gyrom_correction`

Ans d:

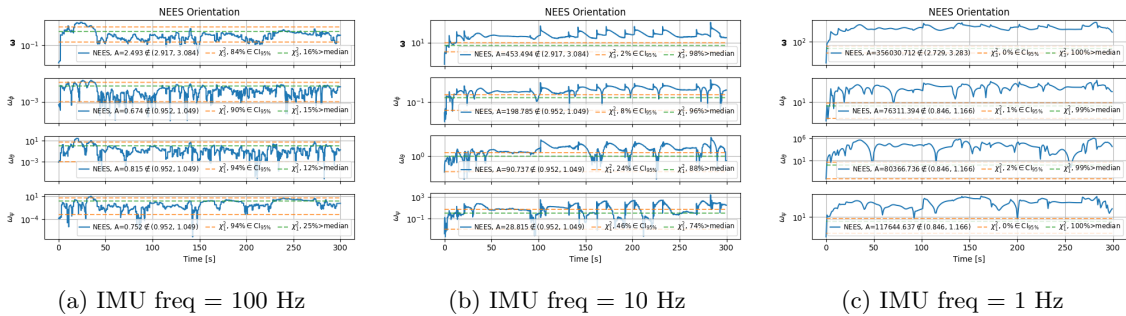
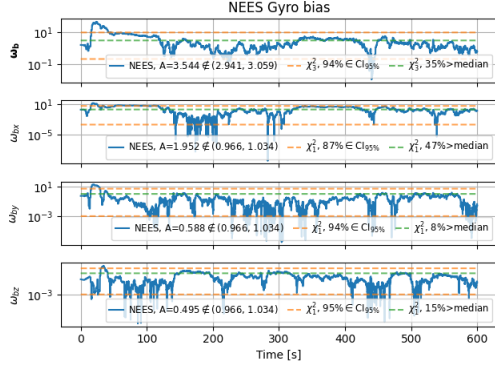


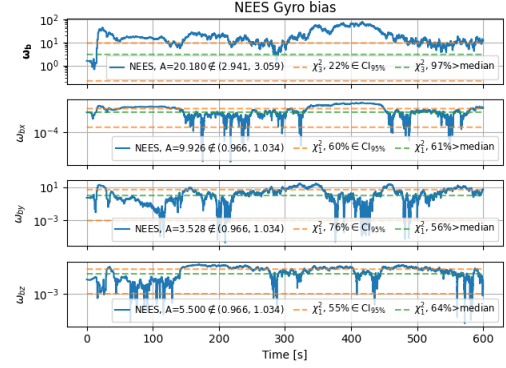
Figure 4: Graphs showing the affects of downsizing IMU measurement frequency on Orientation NEES graph

While changing the tuning parameters, we started by downsizing the frequency of IMU measurements to grasp the importance of sensor data over various states. We tried with the IMU measurement frequencies 100 Hz, 10 Hz, and 1 Hz which progressively worsened the filter performance as seen in the total RMSE values in figure 4. This shows the reliance of the ESKF over the IMU measurement. Lower frequency results in accumulated drift over a longer time, which the

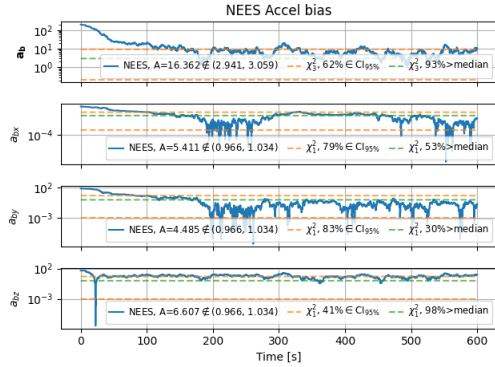
filter struggles to overcome. Since the frequency of GNSS remained constant, the effect on less dynamic states like position remained significantly less than the effect on velocity and orientation. The position drift is only notable in z-direction when both the IMU and GNSS frequencies are 1 Hz or lower as altitude is less dependent on GNSS data and the impact of errors in more dynamic states affects it notably over time.



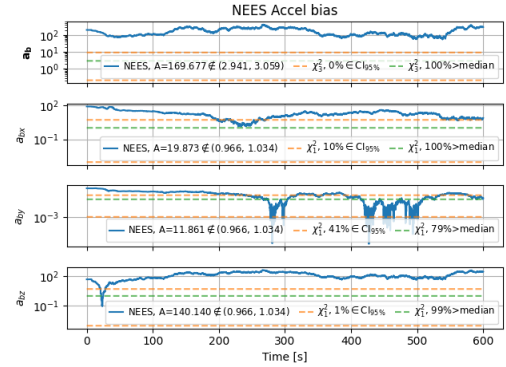
(a) NEES Gyro bias for Gyro Bias noise ($\sigma_{g,b}$) = $1e-5$



(b) NEES Gyro bias for Gyro Bias noise ($\sigma_{g,b}$) = $1e-6$



(c) NEES Accel bias for Accel bias noise ($\sigma_{a,b}$) = $1e-3$



(d) NEES Accel bias for Accel bias noise ($\sigma_{a,b}$) = $1e-4$

Figure 5: Graphs showing the effects of Accelerometer bias noise and Gyro bias noise

For the accel and gyro bias noise parameters, increasing yielded poor results. This was somewhat expected since the data appeared to possess low bias noise. On the other hand, if we slightly decrease the gyro bias standard deviation from $5e-5$ to $1e-5$ or the accel bias standard deviation from $4e-3$ to $1e-3$, the estimation appears to be better for a timescale of 600sec, as in figure 5(a)(c) respectively. This suggests to the filter that the biases are more stable which is also observable in the Accel and Gyro bias ground truth. However, decreasing the bias noises further worsened the filter performance as the filter might have gotten overconfident about the biases as seen in figure 5(b)(d).

Any reasonable increase or decrease in the nominal accel or gyro noise does not have any significant results in shorter timescales (up to 300 sec) thus suggesting that the filter has a good mechanism to handle variation in sensor noise. If we modify the initial state and standard deviation such that the initialization of the filter is less accurate, we expect it to show a larger error at the beginning as the filter tries to stabilize it gradually. To test this, we changed the initial position from $[0.2, 0, -5]$ to $[5.0, -3.0, -10.0]$ and the initial orientation from $[0,0,0]$ to $[0.1,0.1,0.1]$. Since these values are inaccurate, we also increased the position and velocity error standard deviation from 2 to 3 and 0.1 to 0.5 respectively. The results in Figure 6 satisfy our hypothesis as the filter shows large inaccuracies in the beginning (up to 50 sec) and gradually as the measurement refines the state estimates, the filter converges.

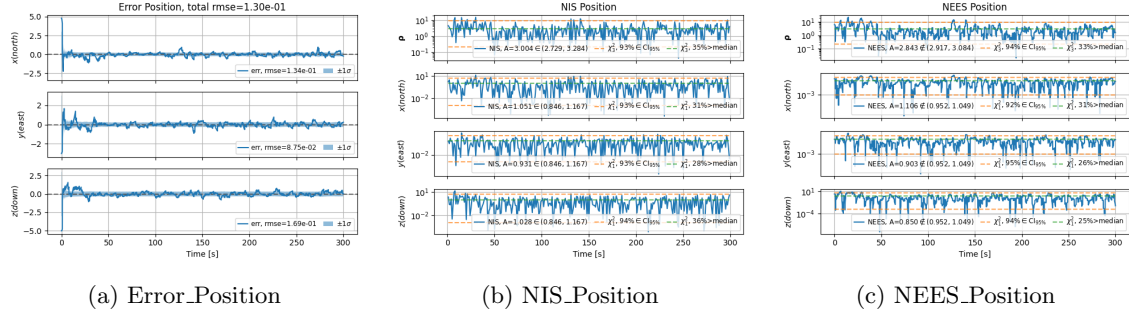


Figure 6: Graphs showing the effects of inaccurate initialization on position estimate.

2 ESKF on Real data

Ans a:

When we are given UAV data with a SIM300 IMU and two Ublox-8 GNSS sensors, it is very important to handle their different update rates while fusing them for ESKF. We can propose 2 strategies to solve this frequency issue.

Firstly, we can use the high-frequency IMU data in ESKF to propagate state and covariance. When the GNSS measurement arrives, we can use interpolation to find the precise IMU state at the GNSS time stamp and use this interpolated state with GNSS measurement for the update step in ESKF.

Alternatively, if the GNSS measurement arrives between 2 IMU time steps, we can store the GNSS measurement and perform the update at the next IMU measurement. We would have to adjust the measurement model to account for the time delay.

Ans b:

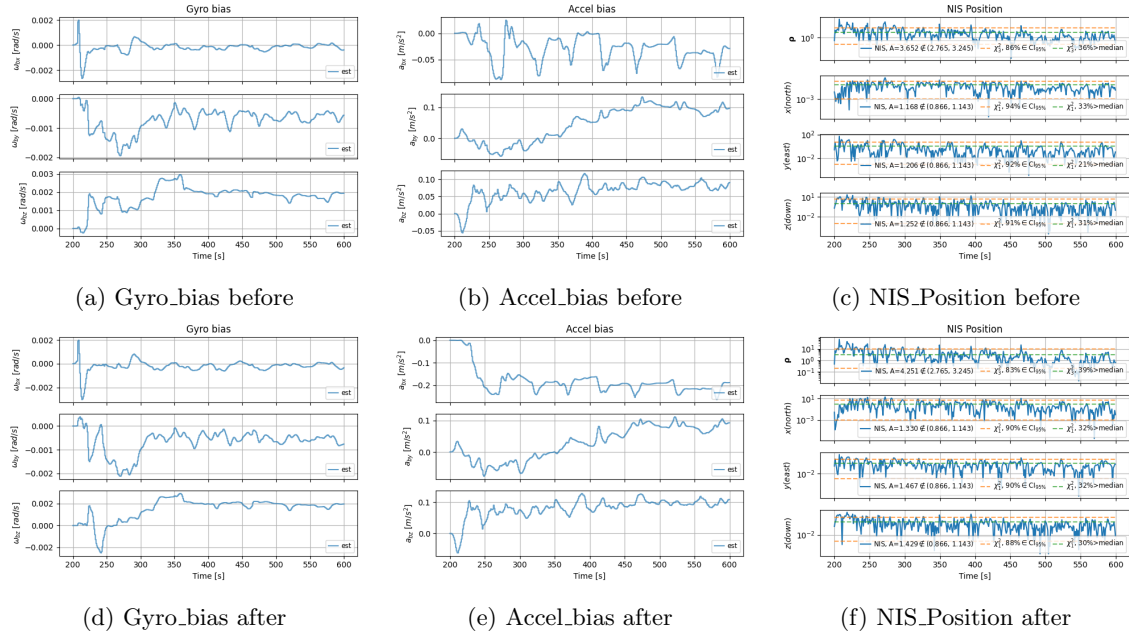


Figure 7: Graphs showing the effects of rounding off accm correction and gyrom correction

Since this is real data and we do not have access to the ground truths, we observe minor variations in gyro and accel bias after we round off accm correction and gyrom correction as can be seen in

figure 7. There are visible differences in bias estimation up to 250 sec after which the filter manages to converge. The NEES position graph shows that the filter performs pretty well before and after corrections, as it remains bounded by the confidence interval almost all the time in both cases. If the incorrectness of the measurement is not previously known, then it is almost impossible to figure it out from the graphs. This suggests that ESKF is pretty robust to the minor real-world impreciseness. This might be because real IMUs like STIM300 are often factory-calibrated to account for scale and mounting errors. Additionally, the real-world data contains a lot of inherent noise, which can mask the effect of small inaccuracies introduced by the rounding of correction matrices. Moreover, as the frequency of IMU measurements is 250Hz, which is significantly higher than the simulation, also boosts the reliability of the filter.

Ans c:

We start exploring different parameters by decreasing the frequency of the GNSS sensor from 1Hz to 0.5Hz to 0.2Hz. We also increase the GNSS noise in the NED direction to simulate real-world conditions and make GNSS measurement less reliable. As the position correction becomes less frequent, the system depends more on IMU for position estimation. As shown in figure 8, the ESKF shows more drift in position estimate, especially in challenging maneuvers due to the accumulated error of IMU. This setup simulates real-world implications such as signal loss, low accuracy, etc.

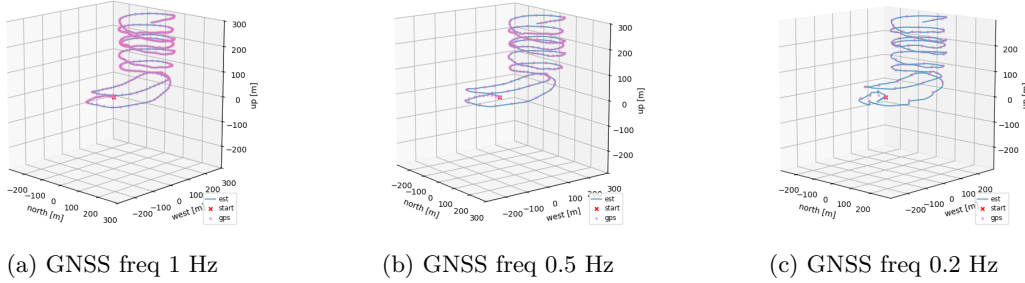


Figure 8: Graphs showing the effect of reducing GNSS update rate in 3D Position

To simulate a poorly calibrated or cheaper IMU, we increased the accelerometer and gyro bias noises to $1e-2$ and $1e-3$ respectively. We also increased the initial accel and gyro bias to 0.2 and 0.1, thus increasing the variability of the system as can be seen in figure 9(a)(b). However, the NIS of the position estimate remains in the confidence bound which suggests that the filter is able to handle high variability in the biases as well.

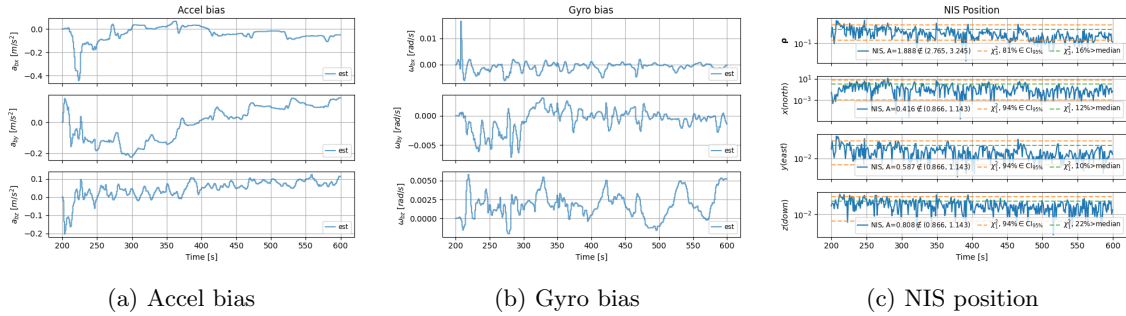
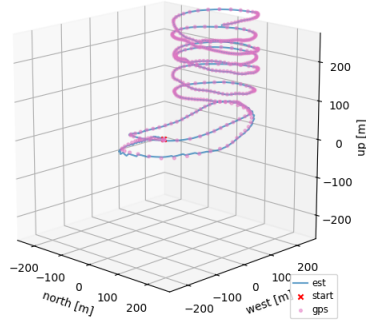


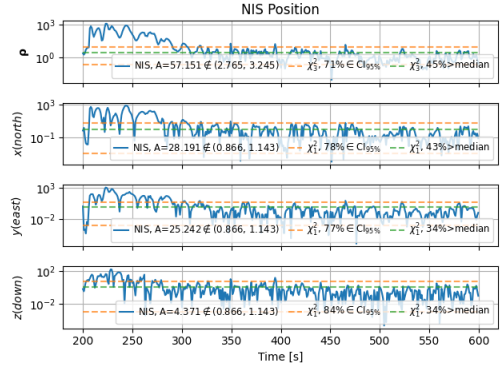
Figure 9: Graphs showing the effect of increased IMU bias noises

The final real-world test is performed with a nonaccurate initial position and orientation. This is relevant for drones and AUVs where the starting position and orientation can vary a lot. We initialize the filter at position and orientation as $[5, 5, -5]$ and $[0, 0, \pi]$ instead of $[1, 0, -1.5]$ and $[0, 0, \frac{\pi}{2}]$ respectively. With poor initial guesses, we assume the filter will need more time to converge, which is validated by figure 10(b). The RMSE is higher than the confidence bound up to the first 300

sec and then gradually stabilizes. Also, the position estimate, as shown in figure 10(a), appears to be jagged at the beginning and smoothens out slowly afterward as the ESKF catches up.



(a) Position in 3D



(b) NIS position

Figure 10: Graphs showing the effect of inaccurate initialization in position tracking

Bibliography

Brekke, Edmund (Aug. 2024). *Fundamentals of Sensor Fusion: Target Tracking, Navigation and SLAM*. 5th. Unpublished manuscript.